

# Silica-coated and annealed CdS nanowires with enhanced photoluminescence

Shan Liang,<sup>1</sup> Min Li,<sup>2</sup> Jia-Hong Wang,<sup>1</sup> Xiao-Li Liu,<sup>1</sup> Zhong-Hua Hao,<sup>1</sup> Li Zhou,<sup>1,3</sup> Xue-Feng Yu,<sup>1,4</sup> and Qu-Quan Wang<sup>1</sup>

<sup>1</sup>Key Laboratory of Artificial Micro- and Nano-structures of Ministry of Education, School of Physics and Technology, Wuhan University, Wuhan 430072, China

<sup>2</sup>School of Physics and Electronic Engineering, Jiangsu Normal University, Xuzhou 221116, China

<sup>3</sup>zhouli@whu.edu.cn

<sup>4</sup>yxf@whu.edu.cn

**Abstract:** The CdS/SiO<sub>2</sub> core/shell nanowires (NWs) with controlled shell thickness were successfully synthesized and subsequently heat-treated at 500 °C. The influences of silica shell coating and annealing processes on their optical properties have been investigated. Compared with original CdS NWs, the annealed CdS/SiO<sub>2</sub> NWs exhibited an enhanced band-edge emission with slowed photoluminescence lifetime, while the intensity of defect emission decreased. The results were ascribed to the surface passivation and recrystallization by shell coating and annealing. We believe our finding would help improving the optical properties of semiconductor NWs, and facilitate its applications in various realms, such as nanoscale emitter, sensor, and photoelectric device.

©2013 Optical Society of America

**OCIS codes:** (160.6000) Semiconductor materials; (250.5230) Photoluminescence; (300.6500) Spectroscopy, time-resolved.

---

## References and links

1. O. Hayden, R. Agarwal, and C. M. Lieber, "Nanoscale avalanche photodiodes for highly sensitive and spatially resolved photon detection," *Nat. Mater.* **5**(5), 352–356 (2006).
2. C. J. Barrelet, A. B. Greytak, and C. M. Lieber, "Nanowire photonic circuit elements," *Nano Lett.* **4**(10), 1981–1985 (2004).
3. Z. Li, J. Wei, P. Li, L. Zhang, E. Shi, C. Ji, J. Liu, D. Zhuang, Z. Liu, J. Zhou, Y. Shang, Y. Li, K. Wang, H. Zhu, D. Wu, and A. Cao, "Solution-processed bulk heterojunction solar cells based on interpenetrating CdS nanowires and carbon nanotubes," *Nano Res.* **5**(9), 595–604 (2012).
4. Y. Liu, Q. Yang, Y. Zhang, Z. Yang, and Z. L. Wang, "Nanowire piezo-phototronic photodetector: theory and experimental design," *Adv. Mater. (Deerfield Beach Fla.)* **24**(11), 1410–1417 (2012).
5. Y. F. Lin, J. Song, Y. Ding, S. Y. Lu, and Z. L. Wang, "Alternating the output of a CdS nanowire nanogenerator by a white-light-stimulated optoelectronic effect," *Adv. Mater. (Deerfield Beach Fla.)* **20**(16), 3127–3130 (2008).
6. J. S. Jie, W. J. Zhang, Y. Jiang, X. M. Meng, Y. Q. Li, and S. T. Lee, "Photoconductive characteristics of single-crystal CdS nanoribbons," *Nano Lett.* **6**(9), 1887–1892 (2006).
7. C. H. Cho, C. O. Aspetti, M. E. Turk, J. M. Kikkawa, S. W. Nam, and R. Agarwal, "Tailoring hot-exciton emission and lifetimes in semiconducting nanowires via whispering-gallery nanocavity plasmons," *Nat. Mater.* **10**(9), 669–675 (2011).
8. D. Li, J. Zhang, Q. Zhang, and Q. Xiong, "Electric-field-dependent photoconductivity in CdS nanowires and nanobelts: exciton ionization, Franz-Keldysh, and Stark effects," *Nano Lett.* **12**(6), 2993–2999 (2012).
9. Q. Zhang, X. Y. Shan, X. Feng, C. X. Wang, Q. Q. Wang, J. F. Jia, and Q. K. Xue, "Modulating resonance modes and Q value of a CdS nanowire cavity by single Ag nanoparticles," *Nano Lett.* **11**(10), 4270–4274 (2011).
10. J. Puthussery, A. Lan, T. H. Kosel, and M. Kuno, "Band-filling of solution-synthesized CdS nanowires," *ACS Nano* **2**(2), 357–367 (2008).
11. R. Agarwal, C. J. Barrelet, and C. M. Lieber, "Lasing in single cadmium sulfide nanowire optical cavities," *Nano Lett.* **5**(5), 917–920 (2005).
12. A. Pan, S. Wang, R. Liu, C. Li, and B. Zou, "Thermal stability and lasing of CdS nanowires coated by amorphous silica," *Small* **1**(11), 1058–1062 (2005).
13. S. Geburt, A. Thielmann, R. Röder, C. Borschel, A. McDonnell, M. Kozlik, J. Kühnel, K. A. Sunter, F. Capasso, and C. Ronning, "Low threshold room-temperature lasing of CdS nanowires," *Nanotechnology* **23**(36), 365204 (2012).
14. R. F. Oulton, V. J. Sorger, T. Zentgraf, R. M. Ma, C. Gladden, L. Dai, G. Bartal, and X. Zhang, "Plasmon lasers at deep subwavelength scale," *Nature* **461**(7264), 629–632 (2009).

15. X. Duan, Y. Huang, R. Agarwal, and C. M. Lieber, "Single-nanowire electrically driven lasers," *Nature* **421**(6920), 241–245 (2003).
16. H. Lee, K. Heo, J. Park, Y. Park, S. Noh, K. S. Kim, C. Lee, B. H. Hong, J. Jian, and S. Hong, "Graphene–nanowire hybrid structures for high-performance photoconductive devices," *J. Mater. Chem.* **22**(17), 8372–8376 (2012).
17. R. M. Ma, L. Dai, H. B. Huo, W. J. Xu, and G. G. Qin, "High-performance logic circuits constructed on single CdS nanowires," *Nano Lett.* **7**(11), 3300–3304 (2007).
18. T. Dufaux, M. Burghard, and K. Kern, "Efficient charge extraction out of nanoscale Schottky contacts to CdS nanowires," *Nano Lett.* **12**(6), 2705–2709 (2012).
19. M. I. Utama, J. Zhang, R. Chen, X. Xu, D. Li, H. Sun, and Q. Xiong, "Synthesis and optical properties of II–VI 1D nanostructures," *Nanoscale* **4**(5), 1422–1435 (2012).
20. B. Piccione, C. H. Cho, L. K. van Vugt, and R. Agarwal, "All-optical active switching in individual semiconductor nanowires," *Nat. Nanotechnol.* **7**(10), 640–645 (2012).
21. Z. X. Yang, W. Zhong, P. Zhang, M. H. Xu, Y. Deng, C. T. Au, and Y. W. Du, "Controllable synthesis, characterization and photoluminescence properties of morphology-tunable CdS nanomaterials generated in thermal evaporation processes," *Appl. Surf. Sci.* **258**(19), 7343–7347 (2012).
22. D. Xu, Y. Xu, D. Chen, G. Guo, L. Gui, and Y. Tang, "Preparation and characterization of CdS nanowire arrays by DC electrodeposit in porous anodic aluminum oxide templates," *Chem. Phys. Lett.* **325**(4), 340–344 (2000).
23. H. Gai, Y. Wu, L. Wu, Z. Wang, Y. Shi, M. Jing, and K. Zou, "Solvothelmal synthesis of CdS nanowires using L-cysteine as sulfur source and their characterization," *Appl. Phys., A Mater. Sci. Process.* **91**(1), 69–72 (2008).
24. K. B. Tang, Y. T. Qian, J. H. Zeng, and X. G. Yang, "Solvothelmal route to semiconductor nanowires," *Adv. Mater. (Deerfield Beach Fla.)* **15**(5), 448–450 (2003).
25. C. C. Kang, C. W. Lai, H. C. Peng, J. J. Shyue, and P. T. Chou, "Surfactant- and temperature-controlled CdS nanowire formation," *Small* **3**(11), 1882–1885 (2007).
26. Q. Wang, G. Zhao, and G. Han, "Synthesis of single crystalline CdS nanorods by a PVP-assisted solvothelmal method," *Mater. Lett.* **59**(21), 2625–2629 (2005).
27. K. Pal, U. N. Maiti, T. P. Majumder, and S. C. Debnath, "A facile strategy for the fabrication of uniform CdS nanowires with high yield and its controlled morphological growth with the assistance of PEG in hydrothelmal route," *Appl. Surf. Sci.* **258**(1), 163–168 (2011).
28. M. A. Correa-Duarte, M. Giersig, N. A. Kotov, and L. M. Liz-Marzán, "Control of packing order of self-assembled monolayers of magnetite nanoparticles with and without SiO<sub>2</sub> coating by microwave irradiation," *Langmuir* **14**(22), 6430–6435 (1998).
29. X. F. Yu, L. D. Chen, M. Li, M. Y. Xie, L. Zhou, Y. Li, and Q. Q. Wang, "Highly efficient fluorescence of NdF<sub>3</sub>/SiO<sub>2</sub> core/shell nanoparticles and the applications for in vivo NIR detection," *Adv. Mater. (Deerfield Beach Fla.)* **20**(21), 4118–4123 (2008).
30. S. T. Selvan, T. T. Tan, and J. Y. Ying, "Robust, non-cytotoxic, silica-coated CdSe quantum dots with efficient photoluminescence," *Adv. Mater. (Deerfield Beach Fla.)* **17**(13), 1620–1625 (2005).
31. L. K. van Vugt, B. Piccione, C. H. Cho, P. Nukala, and R. Agarwal, "One-dimensional polaritons with size-tunable and enhanced coupling strengths in semiconductor nanowires," *Proc. Natl. Acad. Sci. U.S.A.* **108**(25), 10050–10055 (2011).
32. A. Pan, X. Lin, R. Liu, C. Li, X. He, H. Gao, and B. Zou, "Surface crystallization effects on the optical and electric properties of CdS nanorods," *Nanotechnology* **16**(10), 2402–2406 (2005).
33. P. Liu, V. P. Singh, C. A. Jarro, and S. Rajaputra, "Cadmium sulfide nanowires for the window semiconductor layer in thin film CdS–CdTe solar cells," *Nanotechnology* **22**(14), 145304 (2011).
34. F. Wu, J. Z. Zhang, R. Kho, and R. K. Mehra, "Radiative and nonradiative lifetimes of band edge states and deep trap states of CdS nanoparticles determined by time-correlated single photon counting," *Chem. Phys. Lett.* **330**(3-4), 237–242 (2000).
35. L. Yu, X. F. Yu, Y. Qiu, Y. Chen, and S. Yang, "Nonlinear photoluminescence of ZnO/ZnS nanotetrapods," *Chem. Phys. Lett.* **465**(4-6), 272–274 (2008).

## 1. Introduction

As a one-dimensional wide band gap (2.42 eV) semiconductor, CdS nanowires (NWs) have received considerable attention owing to their attractive optical properties [1–20]. Especially, the stimulated emission and lasing of CdS NWs have blossomed increasingly in recent years, attributed to the efforts from a large number of research groups [10–16]. For example, optically pumped lasing of CdS NWs at 75 K was reported by Lieber and associates in 2005 [11]. Stimulated emission was observed by Pan et al. for the silica coated CdS NWs under high-intensity excitation at room temperature [12]. Low threshold lasing of CdS NWs at room temperature was further revealed by Geburt's group [13]. In addition, electrically pumped CdS NWs laser was also reported by Duan and associates [15], which demonstrated their feasibility for producing integrated electrically driven photonic devices. Based on these interesting optical properties, CdS NWs have been regarded as wonderful optical material for various applications, such as telecommunications, solar cells, highly integrated devices [1–4,16–18].

Based on above considerations, great recent efforts have been devoted to synthesize CdS NWs with high crystallinity and efficient photoluminescence (PL) [19–26]. Hydrothermal method is the most employed route for the preparation of CdS NWs due to some significant advantages such as cost-effective, controllable particle size, low-temperature, and easy-operation techniques [24–27]. However, such as-prepared CdS NWs synthesized by hydrothermal method have defects inevitably owing to the surface absorption of surfactant, ligands, or other groups, which reduce the PL efficiency of the CdS NWs [25–27]. In order to further improve the PL efficiency of the as-prepared CdS NWs, the researchers have suggested several processing methods [28–32]. The typical strategy included growing silica shells to passivate the surface of CdS NWs [28–31]. Annealing is an efficient strategy for surface recrystallization [32,33], however the CdS NWs were often damaged under long-term heating in air due to the surface degradation.

In this paper, we investigated the influences of silica shell coating and annealing processes on the PL of CdS NWs. The CdS/SiO<sub>2</sub> core/shell NWs were synthesized, and annealed at 500 °C for 5 h. Compared with the original CdS NWs, such annealed CdS/SiO<sub>2</sub> core/shell NWs exhibited highly efficient band-edge emission of CdS.

## 2. Experimental section

The original CdS NWs were synthesized by the solvothermal method using ethylenediamine as a solvent [12,24]. In brief, 33.5 mL of ethylenediamine was added to a Teflon-lined stainless-steel autoclave of 45 mL capacity, then 0.0025 mol of cadmium nitrate hexahydrate and 0.002 mol of thiacetamide were dissolved in the above solvent. After stirring for about 10 mins, a viscous gel-like solution was obtained. Then, the Teflon-lined stainless-steel autoclave was sealed and heated without stirring at 180 °C for 24 h. The obtained yellow product was centrifuged (5 mins, 4500 rps) and washed with distilled water and ethanol.

Subsequently, the CdS/SiO<sub>2</sub> core/shell NWs were prepared by a modified Stöber method. 10 mg of the as-prepared CdS NWs was dispersed in the mixed solution containing 10 mL ethanol, 450 μL distilled water, and 325 μL of 28% ammonia. Then, 35 μL of TEOS was added to the above mixture and sonicated for about 2 h at room temperature. A white-yellow precipitate was obtained by centrifugation at 4000 rpm, and then re-dispersed in ethanol. As thus, the high-yielded and uniform silica coated CdS NWs were successfully synthesized. In this method, the thickness of silica shell could be controlled by the amount of TEOS. In order to study the joint action of silica shell and annealing processes on the optical properties of the CdS NWs, part of the as-prepared sample was annealed at 500 °C in air atmosphere for 5 h.

The transmission electron microscope (TEM) images were obtained with a JEOL 2010 HT transmission electron microscope (operated at 200 kV). The absorption spectra were measured with a Varian Cary 5000 UV-Vis-NIR spectrophotometer. Powder X-ray diffraction (XRD) analyses were performed on a Bruker D8-advance X-ray diffractometer with Cu K $\alpha$  irradiation ( $\lambda = 1.5406 \text{ \AA}$ ). The PL spectra of the samples were recorded using a spectrometer (Spectrapro 2500i, Acton) equipped with a liquid nitrogen cooled CCD (SPEC-10, Princeton). The excitation laser of 400 nm with a pulse width of around 3 ps and a repetition rate of 76 MHz was generated by a mode-locked Ti:sapphire laser (Mira 900, Coherent) equipped with an optical frequency doubling system.

## 3. Results and discussion

### 3.1 Controllable synthesis of CdS/SiO<sub>2</sub> core/shell NWs

The CdS/SiO<sub>2</sub> core/shell NWs with controlled shell thickness were produced in a modified Stöber method which is facile, high-yielded and reproducible. Compared with the typical procedure [12], methanol is replaced by ethanol in our method. Sonic oscillation was used as a stirring method during the synthesizing procedure, which greatly shortens the synthesis period of silica shell. Figure 1 displays the TEM images of the original CdS NWs and CdS/SiO<sub>2</sub> core/shell NWs with different shell thickness. Figure 1(a) shows the low and high magnitude TEM images of original CdS NWs. It can be seen that the diameter of CdS NWs is

about 70 nm. In addition, the CdS/SiO<sub>2</sub> core/shell NWs with different shell thickness could be obtained by changing the amount of TEOS in the synthesis. Typically, when 2.5 μL, 10 μL, and 35 μL of TEOS were used, the shell thickness was 11 nm, 25 nm, and 70 nm, respectively. Their TEM images of the corresponding CdS/SiO<sub>2</sub> core/shell NWs are shown in Figs. 1(b)-1(d). From the images, it also can be seen that the silica shells are uniform and precisely controllable.

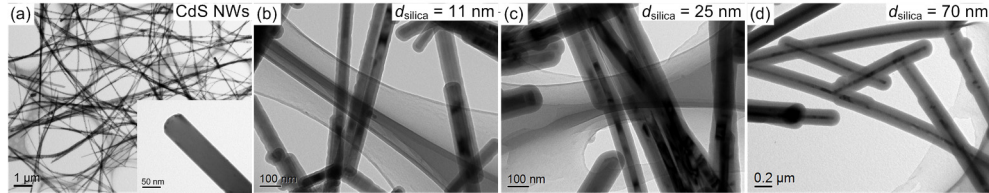


Fig. 1. (a) Low and high magnification TEM images of CdS NWs. (b-d) CdS/SiO<sub>2</sub> core/shell NWs with shell thickness of around (b) 11 nm, (c) 25 nm and (d) 70 nm.

### 3.2 Thermal stability of CdS/SiO<sub>2</sub> core/shell NWs

The XRD patterns of the as-prepared CdS NWs, annealed CdS NWs, CdS/SiO<sub>2</sub> core/shell NWs, and annealed CdS/SiO<sub>2</sub> core/shell NWs are shown in Fig. 2. The annealed CdS NWs have a distinct XRD pattern from the others, which can be indexed as the orthorhombic Cd<sub>3</sub>O<sub>2</sub>SO<sub>4</sub> phase (JCPDS card No.32-0140). It indicated that the structure of CdS NWs is damaged due to the surface degradation (such as oxidation) under long-term heating in air. All the other diffraction peaks in Fig. 2 can be clearly seen and indexed as the hexagonal CdS phase (JCPDS card No.41-1049). Meanwhile, due to the amorphous structure of silica shell, no peaks for silica were detected in the coated sample. The results imply that the silica shell can prevent CdS NWs from being oxidized by oxygen at high temperature, and it offers the feasibility for next optical properties research of CdS NWs under stronger laser excitation.

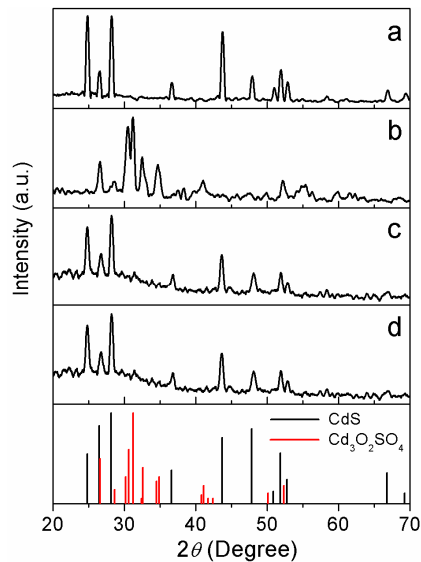


Fig. 2. XRD patterns of (a) CdS NWs, (b) uncoated CdS NWs annealed at 500 °C, (c) CdS/SiO<sub>2</sub> core/shell NWs, and (d) CdS/SiO<sub>2</sub> core/shell NWs annealed at 500 °C.

### 3.3 Optical properties of the annealed CdS/SiO<sub>2</sub> core/shell NWs

The absorption spectra of the as-prepared CdS NWs, CdS/SiO<sub>2</sub> NWs and annealed CdS/SiO<sub>2</sub> core/shell NWs are shown in Fig. 3. All the samples have a pronounced absorption bump at

about 486 nm, which is similar with the results obtained by the other groups [26,27]. By comparing the absorption line shape of the CdS NWs, CdS/SiO<sub>2</sub> NWs, and annealed CdS/SiO<sub>2</sub> NWs, we found that the absorption bump position of CdS NWs is insensitive to the shell coating and annealing processes.

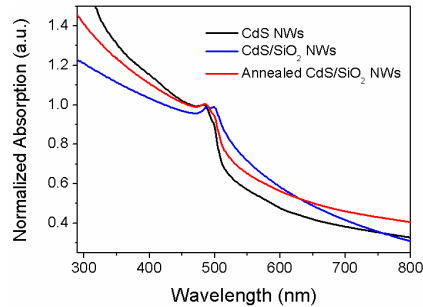


Fig. 3. Normalized absorption spectra of CdS NWs, CdS/SiO<sub>2</sub> NWs, and annealed CdS/SiO<sub>2</sub> core/shell NWs.

The PL spectra of the CdS NWs, CdS/SiO<sub>2</sub> NWs and annealed CdS/SiO<sub>2</sub> NWs are presented in Fig. 4(a). The samples show a sharp emission band at around 505 nm with the excitation of a 400 nm laser, which is attributed to the typical band–band transitions of CdS crystal since the spectral position is very near the band gap of CdS at room temperature [31]. Meanwhile, a broad emission band at around 700 nm can also be observed in these samples, which may be ascribed to structural defects such as crystalline surface structure defects, ionized vacancies and/or impurities [26,27].

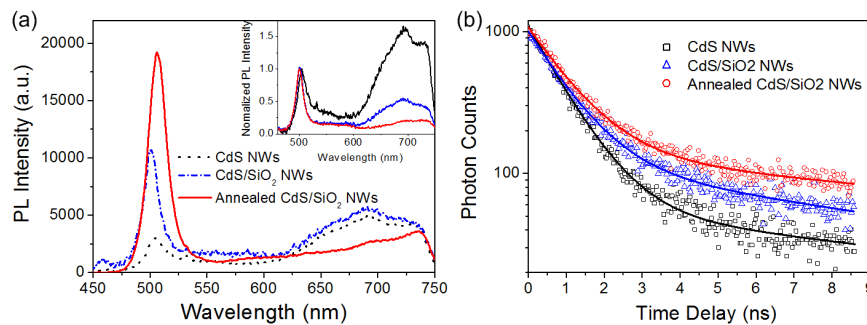


Fig. 4. (a) PL spectra of CdS NWs, CdS/SiO<sub>2</sub> NWs and CdS/SiO<sub>2</sub> NWs annealed at 500 °C. (b) Time-resolved PL of CdS NWs, CdS/SiO<sub>2</sub> NWs and annealed CdS/SiO<sub>2</sub> NWs at ~505 nm.

Most interesting, compared with the original CdS NWs, the band-edge emission of the silica coated CdS NWs enhances nearly 4 times, and that of the annealed CdS/SiO<sub>2</sub> NWs enhances about 8 times. Here, silica coating could passivate the surface of CdS NWs, which prevent the surface adsorption of surfactant, ligands, or other chemical groups. Therefore, it could reduce the number of nonradiative energy channels so as to improve the band-edge emission efficiency. Furthermore, annealing process could improve the crystal quality of CdS NWs under the protection of silica shell. Then the defect (trap) emission was depressed and the band-edge emission efficiency was further enhanced. It can be seen that the defect emission at about 700 nm was decreased by nearly 50% when the CdS/SiO<sub>2</sub> NWs were annealed at 500 °C, which also reveals the improvement of CdS crystal quality. In addition, the full width at half maximum (FWHM) of the band-edge emission peaks for the CdS NWs, CdS/SiO<sub>2</sub> NWs, and annealed CdS/SiO<sub>2</sub> NWs are 20 nm, 17 nm, and 16 nm, respectively. It demonstrates that both the shell coating and annealing processes induce the decreased FWHM of the band-edge emission, which indicate that the trap density near band edge decreases and the quality factor of band-edge emission increases.

To further investigate the dynamics of the band-edge emission, time-resolved PL experiments were performed. As shown in Fig. 4(b), two decay processes with fast lifetime ( $\tau_f$ ) and slow lifetime ( $\tau_s$ ) were observed for the CdS NWs, CdS/SiO<sub>2</sub> NWs and annealed CdS/SiO<sub>2</sub> NWs. We have fitted the PL decay rate of the samples by double exponential, and the fitted values of  $\tau_f$  are 0.86 ns (94%), 0.95 ns (89%) and 0.99 ns (85%) for the CdS NWs, CdS/SiO<sub>2</sub> NWs, and annealed CdS/SiO<sub>2</sub> NWs, respectively. The decrease of density of trap states was expected to reduce the exciton-trap interaction and thus increase the observed lifetime [34,35]. The increased lifetime of band-edge emission for annealed CdS/SiO<sub>2</sub> NWs coincided with their enhanced emission efficiency induced by surface passivation and crystal improvement.

Figure 5(a) displays the excitation power ( $P_{exc}$ ) dependence of the PL intensity ( $I_{PL}$ ) at around 505 nm of the samples. From these data, the slopes ( $\nu = \partial \log I_{PL} / \partial \log P_{exc}$ ) are fitted as 1.56, 1.76 and 1.82 for the original CdS, CdS/SiO<sub>2</sub> and annealed CdS/SiO<sub>2</sub> NWs, respectively. It can be seen that, with the increasing of excitation power, the PL intensity of CdS/SiO<sub>2</sub> NWs and annealed CdS/SiO<sub>2</sub> NWs increase nonlinearly. In contrast, as shown in Fig. 5(b), the defect emission at about 700 nm is nearly linear with slopes of 1.10, 1.19 and 1.11 for the original CdS NWs, CdS/SiO<sub>2</sub> NWs and annealed CdS/SiO<sub>2</sub> NWs, respectively.

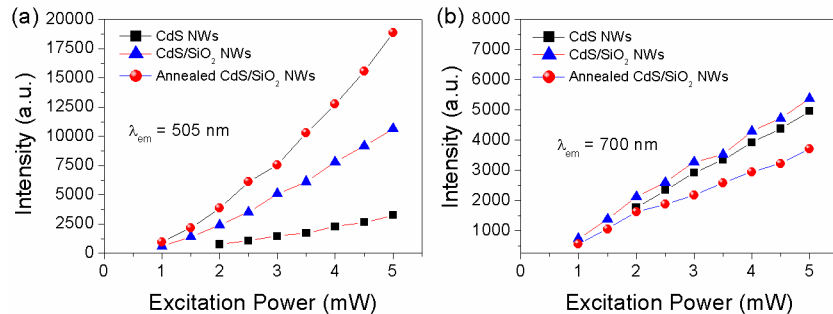


Fig. 5. Excitation power dependence of PL intensity for CdS NWs, CdS/SiO<sub>2</sub> core/shell NWs and annealed CdS/SiO<sub>2</sub> core/shell NWs at (a) 505 nm and (b) 700 nm with excitation wavelength of 400 nm.

#### 4. Conclusion

In summary, the thickness-controlled CdS/SiO<sub>2</sub> core/shell NWs have been successfully prepared in an improved Stöber method, and the influences of silica shell coating and annealing processes on their optical properties have been investigated. The band-edge emission of the annealed CdS/SiO<sub>2</sub> NWs was enhanced with slowed lifetime, and the defect emission was depressed. The results indicated that the joint action of silica coating and annealing processes was beneficial for the band-edge emission efficiency, owing to that silica coating could reduce the nonradiative energy channels by the surface state, and annealing process could improve the crystal quality. We believe our finding would help improving the optical properties of semiconductor NWs, and facilitate its applications in various realms, such as nanoscale emitter, sensor, and photoelectric device.

#### Acknowledgments

This work was supported in part by NSFC (61008043, 11174229 and 11204221), Specialized Research Fund for the Doctoral Program of Higher Education of China (20100141120041) and the National Program on Key Science Research of China (2011CB922201).